The synthesis, structure, and H/D exchange reactions of water-soluble half-sandwich ruthenium(II) hydrides of indenyl and dihydropentalenyl

*Jocelyn P. Lanorio,[a] Charles A. Mebi,[b] Brian J. Frost**

Department of Chemistry, University of Nevada, Reno, NV 89557-0216.

[a] Department of Chemistry, Illinois College, Jacksonville, IL 62650.

[b] Present Address: Department of Physical Sciences, Arkansas Tech University, Russellville, AR 72801, USA

Supporting Information

Tables

Table S-1.	Table S1. Crystallographic Data for IndRu(PTA)$_2$H, IndRu(PTA)$_2$Cl, and [IndRu(PTA)$_3$]$^+$Cl$^-$.	S2
Table S-2	Experimental (X-ray) and Calculated (DFT) Selected Bond Lengths [Å] and Angles [°] for IndRu(PTA)$_2$H (**1**).	S3

Figures

Figure S-1	Aqueous solution of IndRu(PTA)$_2$H under nitrogen is shown in the left NMR tube. On the right is the same solution after exposure to air (right tube).	S3
Figure S-2.	Bottom figure: ^{1}H NMR spectrum of IndRu(PTA)$_2$H in DMSO-d$_6$. Inset shows hydride region. Top figure: Expanded ^{1}H NMR spectrum showing resonances for the indenyl ligand.	S4
Figure S-3.	^{13}C{^{1}H} NMR of IndRu(PTA)$_2$H in DMSO-d$_6$.	S5
Figure S-4.	High resolution ESI-MS+ of IndRu(PTA)$_2$H in methanol. Inset shows computer generated spectrum of IndRu(PTA)$_2$H.	S5
Figure S-5	^{31}P NMR spectrum of DpRu(PTA)$_2$H in DMSO-d_6.	S6
Figure S-6	^{31}P{^{1}H} NMR spectrum of DpRu(PTA)$_2$H in D$_2$O. The bottom spectrum is prior to exchange the top spectrum is after ~30 minutes in D$_2$O.	S6
Figure S-7.	IR Spectrum of solid IndRu(PTA)$_2$H, $\nu_{Ru\text{-}H}$ is indicated by arrow.	S7
Figure S-8.	IR spectra of DpRu(PTA)$_2$H (red/bottom) and DpRu(PTA)$_2$D (blue/top). The arrows indicate $\nu_{Ru\text{-}H}$ and $\nu_{Ru\text{-}D}$.	S7
Figure S-9.	^{13}C{^{1}H} NMR Spectrum of IndRu(PTA)$_2$Cl in CDCl$_3$.	S8
Figure S-10.	High resolution ESI-MS+ of IndRu(PTA)$_2$Cl in methanol. Inset shows computer generated spectrum of IndRu(PTA)$_2$Cl.	S8
Figure S-11.	Arrhenius Plot for the H/D Exchange between IndRu(PTA)$_2$H and D$_2$O.	S9
Figure S-12	Kinetics of the Reaction of IndRu(PTA)$_2$D and H$_2$O as monitored by ^{31}P{^{1}H} NMR spectroscopy. The resonance for IndRu(PTA)$_2$D (triplet) disappears as the singlet for IndRu(PTA)$_2$H appears over time.	S10
Figure S-13	Proposed mechanism for H/D exchange.	S10
Figure S-14	Hydride region of the ^{1}H NMR spectrum (toluene-d_8) showing the formation of IndRu(PTA)$_2$H from the reaction of IndRu(PTA)(PPh$_3$)H and PTA at 80 °C.	S11

Table S1. Crystallographic Data for $IndRu(PTA)_2H$, $IndRu(PTA)_2Cl$, and $[IndRu(PTA)_3]^+Cl^-$.

	$IndRu(PTA)_2H$ (1)	$IndRu(PTA)_2Cl$ (3)	$[IndRu(PTA)_3]^+Cl^-$	$DpRu(PTA)_2H$ (2)
Empirical formula	$C_{24}H_{40}N_6O_{2.5}P_2Ru$	$C_{21}H_{31}ClN_6P_2Ru$	$C_{27}H_{43}ClN_9O_4P_3Ru$	$C_{20}H_{34}N_6P_2Ru$
Formula weight	615.63	565.98	787.13	521.54
Color	Pale yellow	Orange	Yellow	Colorless
T(K)	99(2)	100(2)	100(2)	100(2)
Wavelength (Å)	0.71073	0.71073	0.71073	0.71073
Crystal system	Triclinic	Orthorhombic	Triclinic	Triclinic
Space group	P-1	Pbca	P-1	P-1
a (Å)	6.2430(3)	18.0195(2)	11.2115(4)	9.4855(5)
b (Å)	11.8570(6)	12.50350(10)	11.6519(4)	10.9815(6)
c (Å)	19.1640(11)	40.1336(3)	15.2008(5)	10.9853(6)
α (deg)	72.292(3)	90	111.748(2)	81.574(2)
β (deg)	88.761(3)	90	90.671(2)	77.656(2)
γ (deg)	80.844(3)	90	114.265(2)	71.825(2)
Volume (Å^3)	1333.61(12)	9042.37(14)	1649.64(10)	1058.12(10)
Z	2	16	2	2
D_{calcd} (Mg/m^3)	1.533	1.663	1.585	1.637
Abs coeff (mm^{-1})	0.744	0.976	0.751	0.913
Crystal size (mm^3)	0.35 × 0.09 × 0.07	0.13 × 0.09 × 0.08	0.26 × 0.08 × 0.05	0.31 × 0.13 × 0.04
θ range (deg)	1.83 to 30.10	1.01 to 30.07	1.47 to 30.06	1.90 to 26.00
Index ranges	$-8 \le h \le 8$ $-16 \le k \le 16$ $-26 \le l \le 26$	$-25 \le h \le 14$ $-17 \le k \le 17$ $-56 \le l \le 56$	$-15 \le h \le 15$ $-16 \le k \le 16$ $-21 \le l \le 21$	$-11 \le h \le 11$ $-13 \le k \le 13$ $-13 \le l \le 13$
reflns collected	34428	216802	63467	12594
indep reflns	7767 R_{int} = 0.0451	13259 R_{int} = 0.0878	9588 R_{int} = 0.0400	4079 R_{int} = 0.0561
abs correction	SADABS	SADABS	SADABS	SADABS
data/restr/para	7767/0/330	13259/0/559	9588/0/388	4079/0/266
GOF on F^2	1.128	1.051	1.048	1.062
final R indices [I>2σ(I)]	R_1 = 0.0449 wR_2 = 0.1114	R_1 = 0.0387 wR_2 = 0.0724	R_1 = 0.0705 wR_2 = 0.2044	R_1=0.0456 wR_2=0.0871
R indices (all data)	R_1 = 0.0498 wR_2 = 0.1138	R_1 = 0.0654 wR_2 = 0.0839	R_1 = 0.0792 wR_2 = 0.2132	R_1=0.0690 wR_2=0.1004
CCDC #	1896057	1896059	1896056	1896058

Table S-2. Experimental (X-ray) and Calculated (DFT) Selected Bond Lengths [Å] and Angles [°] for IndRu(PTA)$_2$H (**1**).

	X-ray	DFT
Ru-H	1.53(4)	1.59
Ru-P(1)	2.2362(7)	2.366
Ru-P(2)	2.2343(7)	2.364
Ru-C(13)	2.347(3)	2.528
Ru-C(14)	2.238(3)	2.299
Ru-C(15)	2.219(3)	2.253
Ru-C(16)	2.237(3)	2.301
Ru-C(17)	2.340(3)	2.529
Ru-Cp_{cent}	1.926	2.040
P(1)-Ru-P(2)	98.51(3)	97.15
P(1)-Ru-H	82.8(14)	84.60
P(2)-Ru-H	79.8(14)	84.30

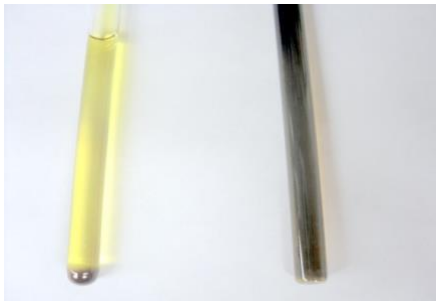

Figure S-1. Aqueous solution of IndRu(PTA)$_2$H under nitrogen is shown in the left NMR tube. On the right is the same solution after exposure to air (right tube).

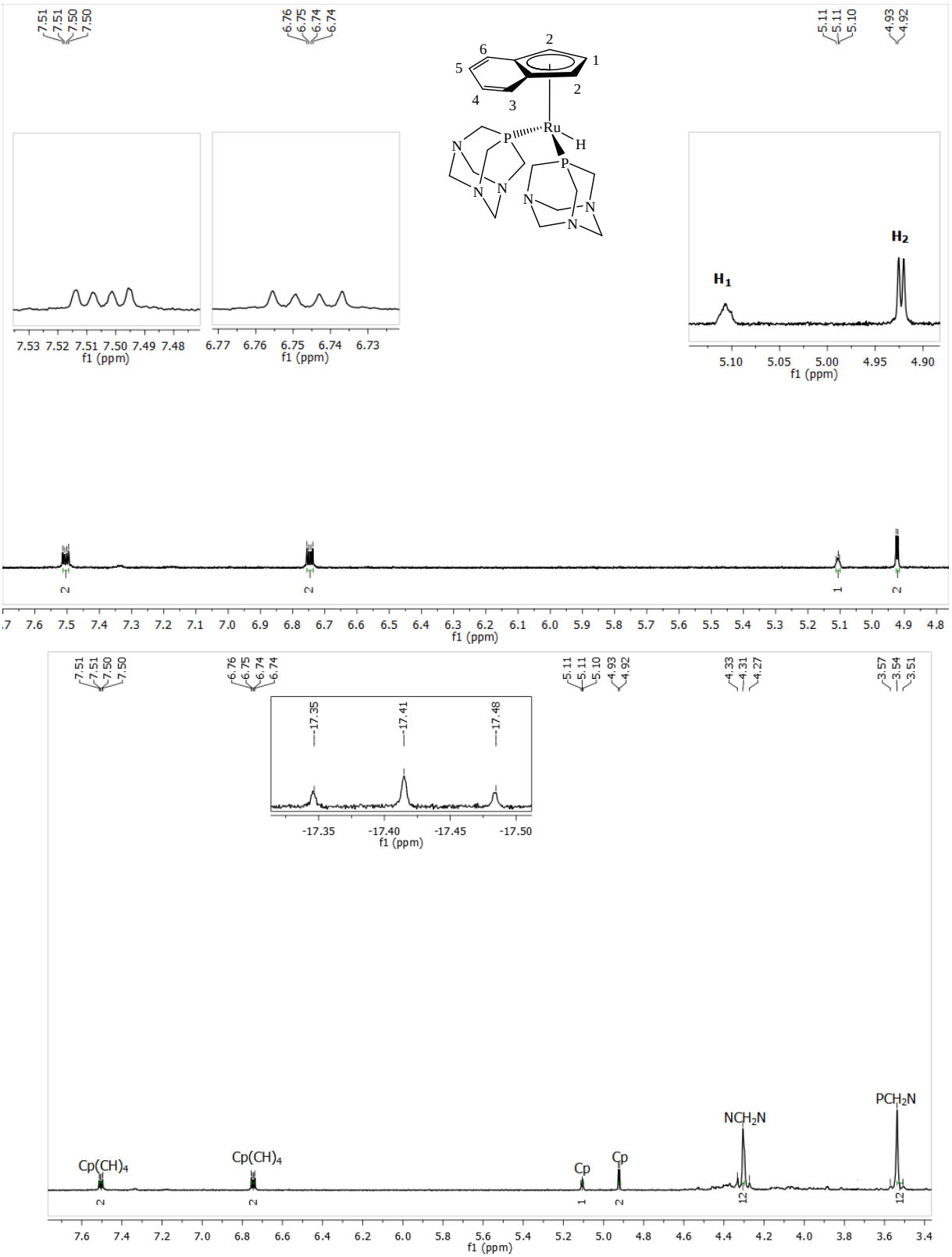

Figure S-2. Bottom figure: ^{1}H NMR spectrum of IndRu(PTA)$_2$H in DMSO-d$_6$. Inset shows hydride region. Top figure: Expanded ^{1}H NMR spectrum showing resonances for the indenyl ligand.

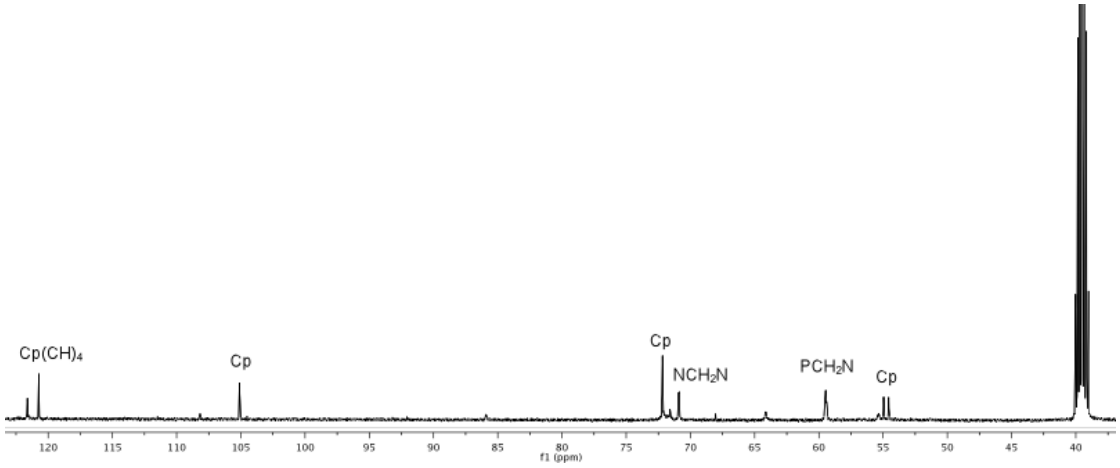

Figure S-3. $^{13}C\{^{1}H\}$ NMR of IndRu(PTA)$_2$H in DMSO-d$_6$.

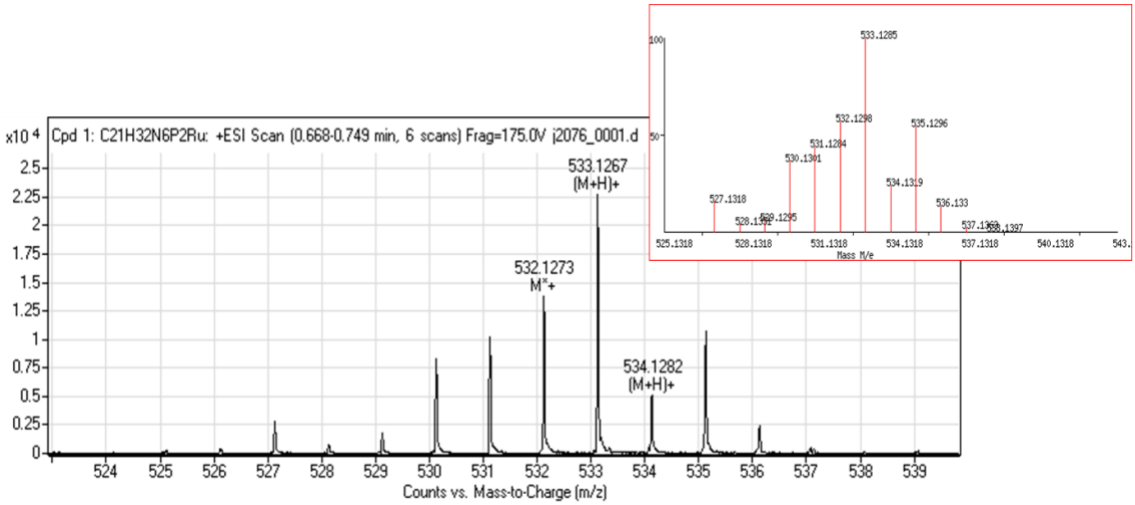

Figure S-4. High resolution ESI-MS+ spectrum of IndRu(PTA)$_2$H in methanol. Inset shows computer generated spectrum of IndRu(PTA)$_2$H.

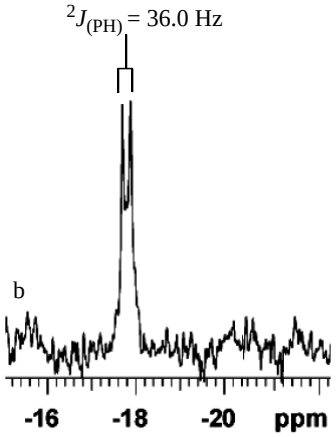

Figure S-5. ^{31}P NMR spectrum of DpRu(PTA)$_2$H in DMSO-d_6.

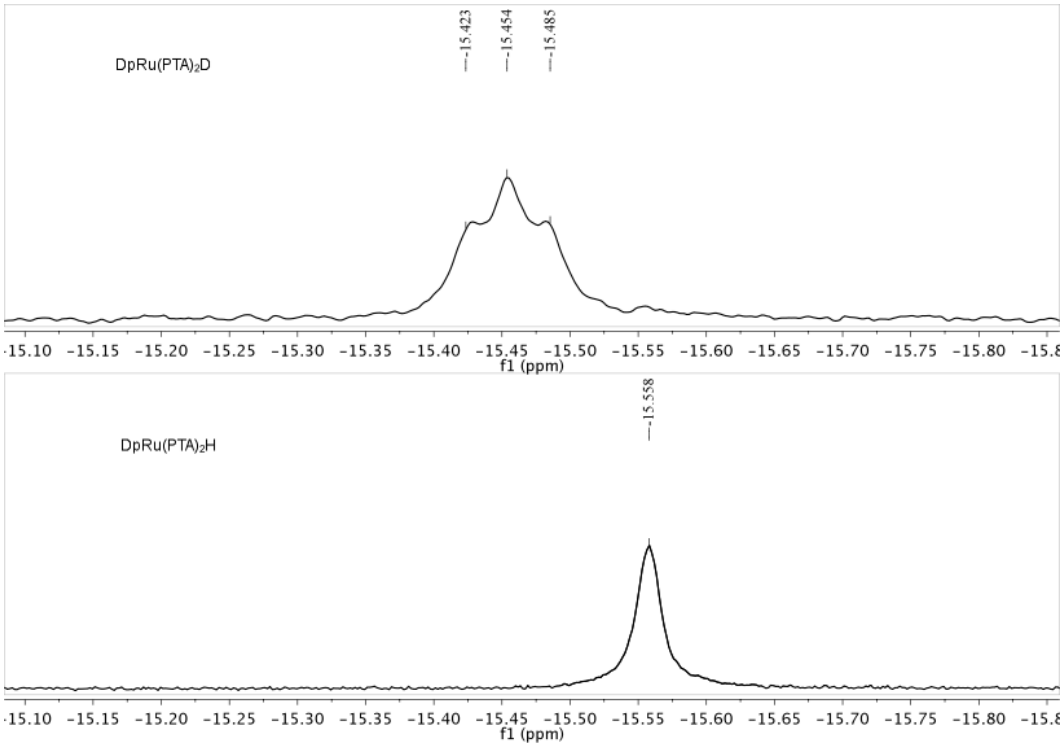

Figure S-6. $^{31}P\{^1H\}$ NMR spectrum of DpRu(PTA)$_2$H in D_2O. The bottom spectrum is prior to exchange the top spectrum is after ~30 minutes in D_2O.

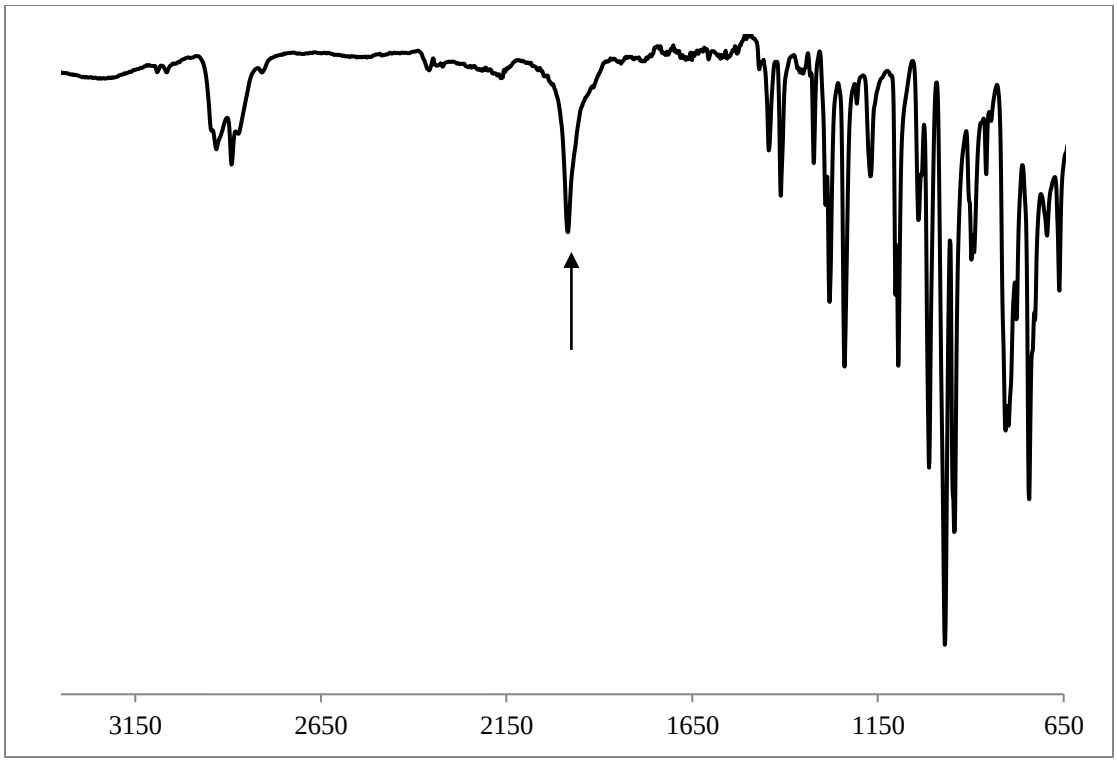

Figure S-7. IR Spectrum of solid IndRu(PTA)$_2$H, $\nu_{Ru\text{-}H}$ is indicated by arrow.

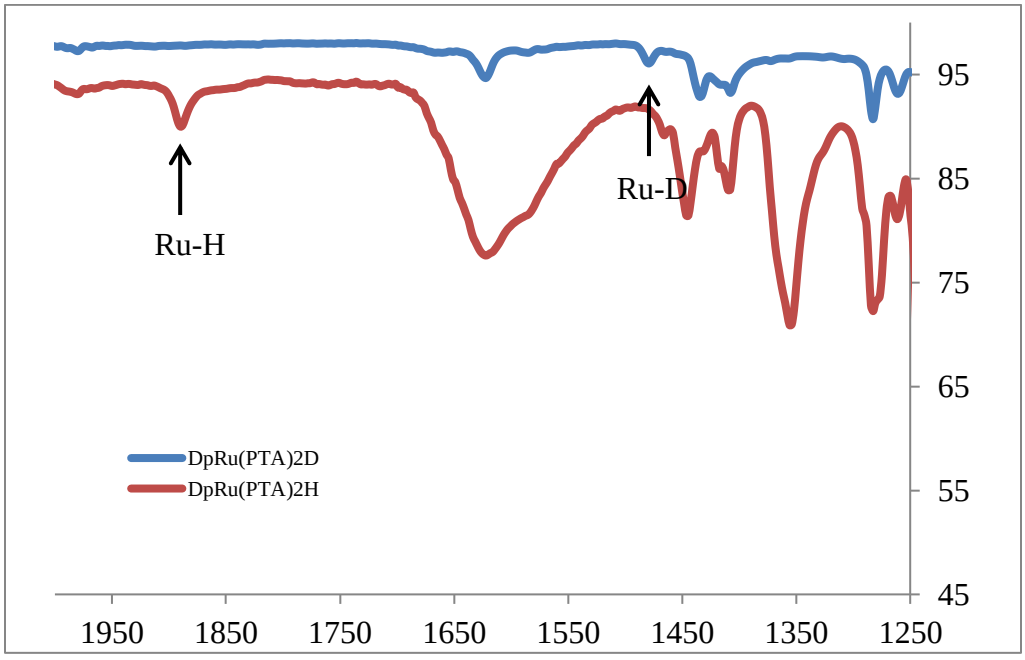

Figure S-8. IR spectra of DpRu(PTA)$_2$H (red/bottom) and DpRu(PTA)$_2$D (blue/top). The arrows indicate $\nu_{Ru\text{-}H}$ and $\nu_{Ru\text{-}D}$.

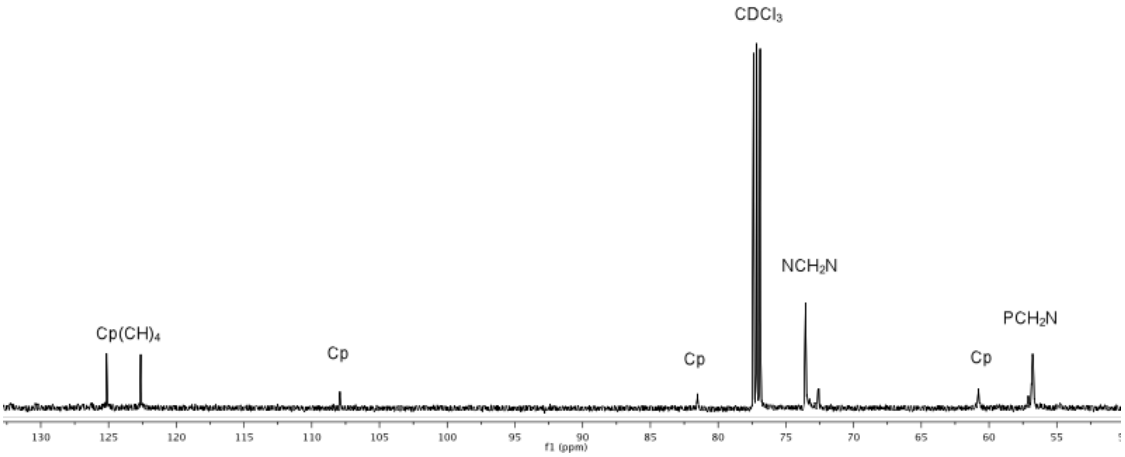

Figure S-9. $^{13}C\{^{1}H\}$ NMR Spectrum of IndRu(PTA)$_2$Cl in $CDCl_3$.

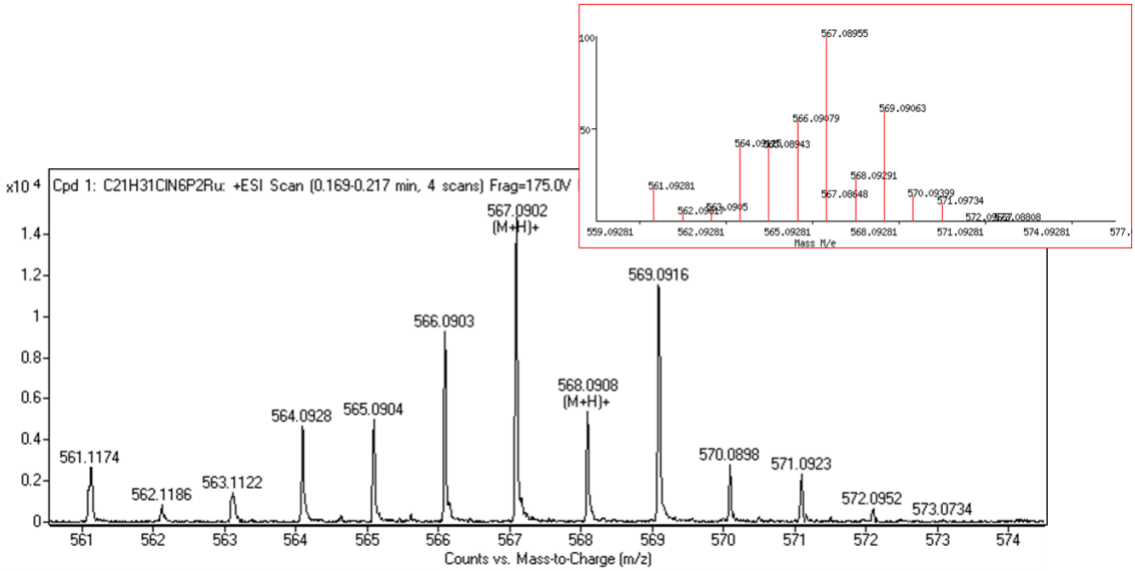

Figure S-10. High resolution ESI-MS+ of IndRu(PTA)$_2$Cl in methanol. Inset shows computer generated spectrum of IndRu(PTA)$_2$Cl.

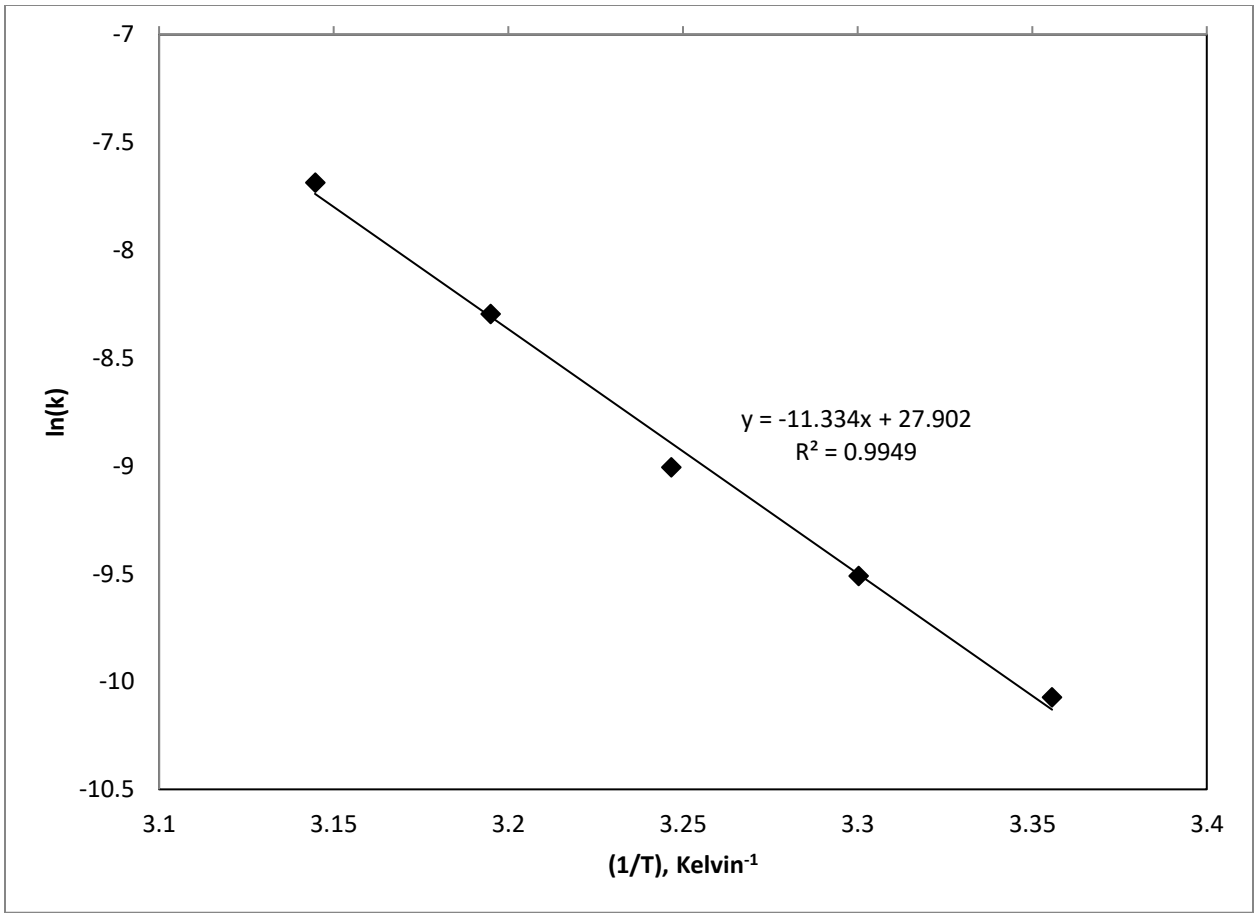

Figure S-11. Arrhenius Plot for the H/D Exchange between IndRu(PTA)$_2$H and D_2O.

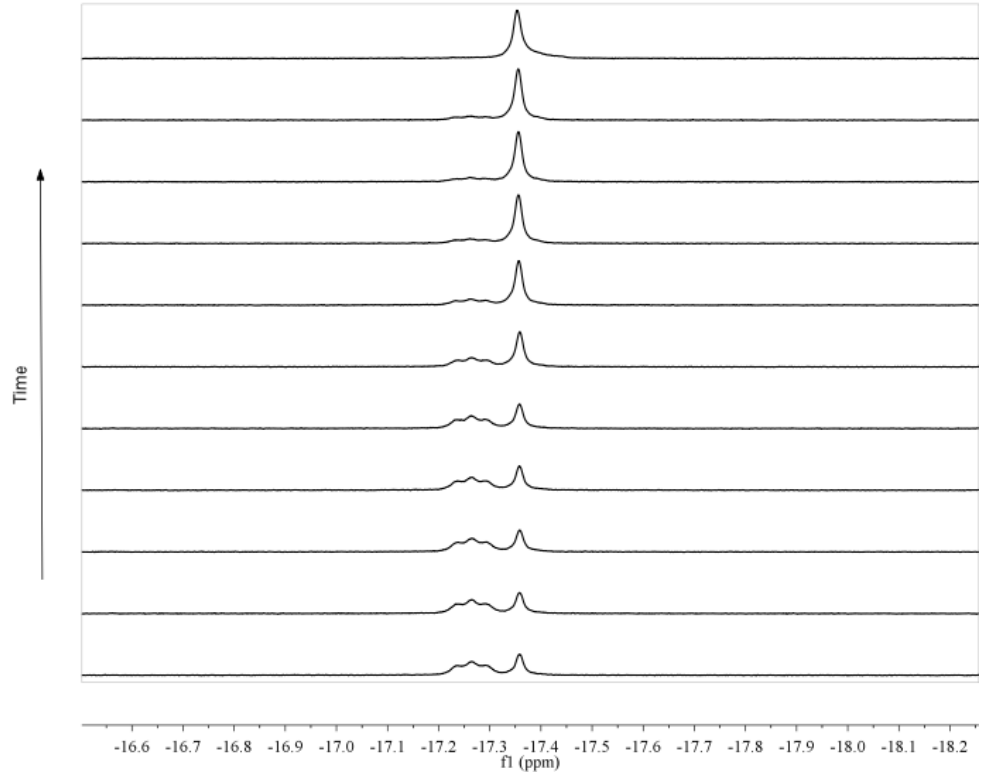

Figure S-12. Kinetics of the Reaction of IndRu(PTA)$_2$D and H_2O as monitored by $^{31}P\{^1H\}$ NMR spectroscopy. The resonance for IndRu(PTA)$_2$D (triplet) disappears as the singlet for IndRu(PTA)$_2$H appears over time.

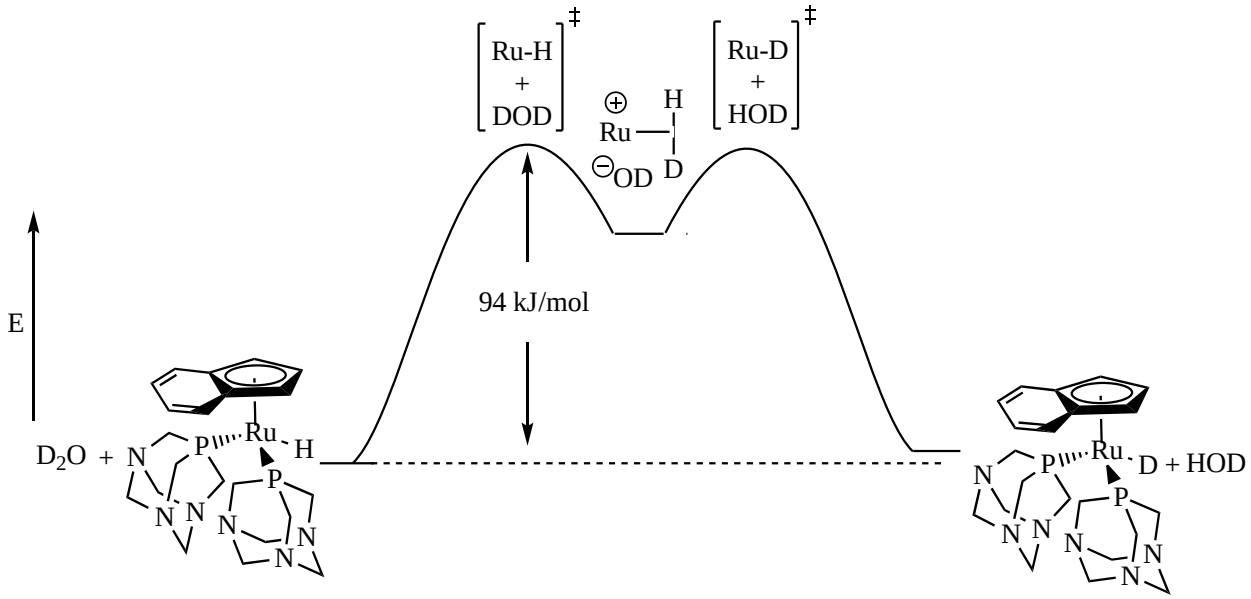

Figure S-13. Proposed mechanism for H/D exchange.

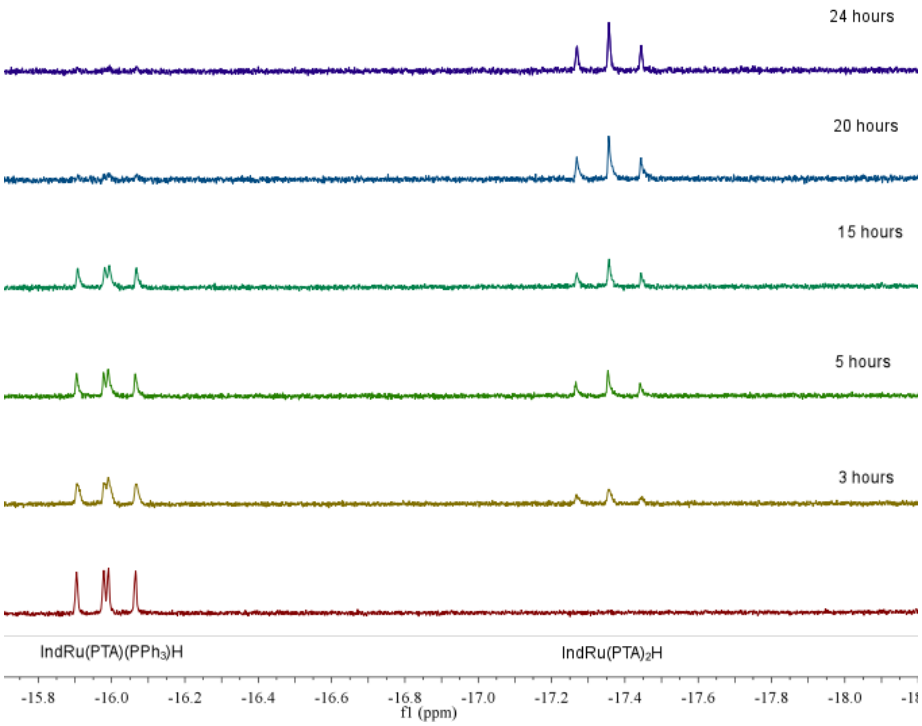

Figure S-14. Hydride region of the ^{1}H NMR spectrum (toluene-d_8) showing the formation of IndRu(PTA)$_2$H from the reaction of IndRu(PTA)(PPh$_3$)H and PTA at 80 °C.